Biodegradation (2010) 21:81–95
DOI 10.1007/s10532-009-9283-x

ORIGINAL PAPER

Can microbially-generated hydrogen sulfide account for the rates of U(VI) reduction by a sulfate-reducing bacterium?

Benjaporn Boonchayaanant · Baohua Gu · Wei Wang · Monica E. Ortiz · Craig S. Criddle

Received: 12 February 2009 / Accepted: 25 June 2009 / Published online: 14 July 2009

Abstract In situ remediation of uranium contaminated soil and groundwater is attractive because a diverse range of microbial and abiotic processes reduce soluble and mobile U(VI) to sparingly soluble and immobile U(IV). Often these processes are linked. Sulfate-reducing bacteria (SRB), for example, enzymatically reduce U(VI) to U(IV), but they also produce hydrogen sulfide that can itself reduce U(VI). This study evaluated the relative importance of these processes for *Desulfovibrio aerotolerans*, a SRB isolated from a U(VI)-contaminated site. For the conditions evaluated, the observed rate of SRB-mediated U(VI) reduction can be explained by the abiotic reaction of U(VI) with the microbially-generated H_2S. The presence of trace ferrous iron appeared to enhance the extent of hydrogen sulfide-mediated U(VI) reduction at 5 mM bicarbonate, but had no clear effect at 15 mM. During the hydrogen sulfide-mediated reduction of U(VI), a floc formed containing uranium and sulfur. U(VI) sequestered in the floc was not available for further reduction.

Keywords Uranium reduction · Sulfate-reducing bacteria · Hydrogen sulfide · Growth kinetics · Ferrous iron

B. Boonchayaanant · C. S. Criddle (✉)
Department of Civil and Environmental Engineering, Stanford University, 473 Via Ortega, Yang and Yamazaki Environment and Energy Building 151, Stanford, CA 94305, USA
e-mail: ccriddle@stanford.edu

B. Gu · W. Wang
Environmental Sciences Division, Oak Ridge National Laboratory, Oak Ridge, TN, USA

M. E. Ortiz
Department of Bioengineering, Stanford University, Stanford, CA, USA

List of symbols

$A_{\text{predicted}}$	Acetate concentration predicted from the stoichiometric ratio of acetate production to ethanol consumption (mM)
A_0	Acetate concentration at the initial time (mM)
C	Covariance matrix
f_{aq}	Fraction of mole of hydrogen sulfide in the aqueous phase
$f_{\text{aq},i-1}$	Fraction of mole of hydrogen sulfide in the aqueous phase on day $i-1$
f_{g}	Fraction of mole of hydrogen sulfide in the gas phase
$f_{\text{H}_2\text{S,aq}}$	Fraction of mole of H_2S in the total mole of hydrogen sulfide in the aqueous phase $= \frac{\text{H}_2\text{S}_{(\text{aq})}}{\text{H}_2\text{S}_{(\text{aq})}+\text{HS}^-_{(\text{aq})}}$
J	Jacobian matrix
k	Pseudo second-order rate constant for ethanol utilization (l/mg protein/day)

k_H	Henry's law constant (atm/mol fraction)
M_T	Total mole of hydrogen sulfide in a serum bottle (mmol)
n	Number of data points for uranium measurements
p	Number of fitting parameters for uranium reduction kinetics
R	Gas constant = 0.08206 $\left(\frac{\text{l·atm}}{\text{mol·K}}\right)$
r_A	Stoichiometric ratio of acetate production to ethanol consumption
$r_{sulfide}$	Stoichiometric ratio of hydrogen sulfide production to ethanol consumption
S	Ethanol concentration (mM)
$S_{measured}$	Measured ethanol concentration (mM)
S_0	Ethanol concentration at the initial time (mM)
$S_{predicted}$	Ethanol concentration predicted from a kinetic model (mM)
$S_{p,\text{mol},i-1}$	Mol of ethanol in a serum bottle on day $i-1$ predicted from a kinetic model and accounted for the ethanol loss due to sampling effect (mmol)
$S_{p,\text{mol},i}$	Mol of ethanol in a serum bottle on day i predicted from a kinetic model (mmol)
SS_{reg}	Sum of the squared errors of the measured values from the values predicted by a model
SS_{tot}	Sum of the squared errors of the measured values from the mean of all measured values
$Sulfide_{p,i}$	Mole of hydrogen sulfide in a serum bottle predicted from the stoichiometric ratio of hydrogen sulfide production to ethanol consumption on day i (mmol)
$Sulfide_{p,i-1}$	Mole of hydrogen sulfide in a serum bottle predicted from the stoichiometric ratio of hydrogen sulfide production to ethanol consumption on day $i-1$ (mmol)
t	Time (d)
T	Absolute temperature (K)
$U(VI)_{in}$	Initial concentration of U(VI) (μM)
X	Protein concentration as proxy of biomass concentration (mg protein/l)
X^{-1}	Inverse of matrix X
X^T	Transpose of matrix X
Y	Biomass yield on ethanol (g protein/mol ethanol)
σ_s^2	Mean square fitting error for improved estimate of measured ethanol data ((mM)^2)
ρ_w	Density of water (kg/m^3)

Introduction

Uranium mining and processing for nuclear weapon production has resulted in widespread uranium contamination of soil and groundwater. When ingested, it is known to cause kidney and liver damage (Taylor and Taylor 1997), leading the US Environmental Protection Agency (EPA) to establish a maximum contaminant level (MCL) in drinking water of 30 ppb. In situ remediation of uranium-contaminated soil and water is attractive because it avoids off-site handling of hazardous materials (McCullough et al. 1999). Many microorganisms, including sulfate-reducing bacteria (SRB), iron-reducing bacteria, and fermenting bacteria, reduce soluble U(VI) species to sparingly soluble U(IV) species, such as solid uraninite (Lovley and Phillips 1992a; Gorby and Lovley 1992; Lovley et al. 1993a, b; Francis et al. 1994; Sani et al. 2002; Anderson and Lovley 2002). Biostimulation of U(VI) reduction is thus a potentially attractive means of immobilizing uranium and preventing it from migration with groundwater (Anderson and Lovley 2002).

A few pilot studies have been conducted to investigate the potential for in situ U(VI) reduction (Anderson et al. 2003; Wu et al. 2006a, b). In tests at the DOE Natural and Accelerated Bioremediation Research Field Research Center (FRC), Oak Ridge, Tennessee, weekly 2-day pulses of ethanol over a period of years stimulated U(VI) reduction to sparingly soluble U(IV) with U(VI) aqueous concentrations below the drinking water standard (Wu et al. 2007). Most probable number (MPN) analyses (Wu et al. 2006b) and clone libraries of sediment samples (Wu et al. 2007; Cardenas et al. 2008; Hwang et al. 2008) indicated that SRB, and especially *Desulfovibrio*-like species, were abundant, as were functional

genes associated with metal reduction (He et al. 2007). During ethanol additions, U(VI) reduction occurred concurrently with sulfate reduction to sulfide, implicating SRB in the field-scale U(VI) reduction (Wu et al. 2006a, b).

During SRB growth, sulfate is reduced to hydrogen sulfide which can abiotically reduce U(VI) to U(IV). In previous studies, Hua et al. (2006), Hua and Deng (2008), and Wersin et al. (1994) observed abiotic U(VI) reduction by both hydrogen sulfide and sulfide-containing minerals. The rates of U(VI) reduction by hydrogen sulfide were rapid at low bicarbonate concentrations (<15 mM at pH 6.89; Hua et al. 2006). However, most previous studies of microbial uranium reduction have evaluated rates of U(VI) reduction in the presence of high concentrations of bicarbonate (20–30 mM); conditions under which U(VI) reduction by hydrogen sulfide is negligible (Elias et al. 2004; Ganesh et al. 1997; Lovley and Phillips 1992a, b; Lovley et al. 1993a, b; Phillips et al. 1995; Pietzsch et al. 1999; Pietzsch and Babel 2003; Spear et al. 1999, 2000). Although the use of high bicarbonate concentrations can ensure stable pH in experimental systems, the resulting conditions are unlike those of most field sites. Bicarbonate levels in typical groundwater are <5 mM. Investigation of U(VI) reduction at high bicarbonate conditions could therefore mask abiotic U(VI) reduction by hydrogen sulfide. To date, no studies have elucidated the relative significance of cell-associated reductants and H_2S for U(VI) reduction under buffer conditions similar to those at field sites. This study addresses that knowledge gap. Two findings were unexpected: increased U(VI) reduction in the presence of trace metals, particularly iron, and a decreased rate and extent of reduction due to the formation of a precipitates containing uranium and sulfur.

Methods

Isolation and cultivation

A sulfate-reducing bacterium was isolated from a sulfate-reducing enrichment initiated with a sample of sediment from an ethanol-fed U(VI)-reducing soil column (Gu et al. 2005). The soil core used for the column experiment came from a well at the DOE Oak Ridge Field Research Center, Oak Ridge, TN (Gu et al. 2005). The isolate was obtained using the deep agar dilution technique (Widdel and Pfennig 1984). The medium for isolation contained: $NaHCO_3$, 0.3 g/l; NH_4Cl, 1.0 g/l; $CaSO_4$, 1.0 g/l; $MgSO_4{\cdot}7H_2O$, 2.0 g/l; $FeSO_4{\cdot}7H_2O$, 0.5 g/l; Yeast extract, 1.0 g/l; ethanol, 0.46 g/l; supplemented with 1% agar, 0.01% sodium ascorbate, and 0.01% sodium thioglycolate. The pure culture was maintained anaerobically in a 150-ml serum bottle under helium headspace at 30°C and transferred to a fresh medium every 7 days. The medium for cultivation contained: Na_2SO_4, 1.66 g/l; ethanol, 0.46 g/l; $NaHCO_3$, 2.5 g/l (30 mM); NaCl, 0.9 g/l; KCl, 0.5 g/l; NH_4Cl, 1 g/l; $MgCl_2{\cdot}6H_2O$, 0.2 g/l; $CaCl_2{\cdot}2H_2O$, 0.02 g/l; $Na_3P_3O_9$, 0.1 g/l; $Na_2S{\cdot}H_2O$, 0.25 g/l; vitamin stock solution I, 1 ml/l; vitamin stock solution II, 1 ml/l; and the trace element stock solution, 10 ml/l. The vitamin stock solution I consisted of hydroxocobalabin hydrochloride, 0.05 g/l; *p*-aminobenzoic acid, 0.2 g/l; biotin, 0.1 g/l; nicotinic acid, 0.35 g/l; L-pantothenic acid-hemicalcium salt, 0.1 g/l; pyrodoxin monohydrochloride, 0.1 g/l; and thiamin hydrochloride, 0.3 g/l. The vitamin stock solution II consisted of folic acid-$2H_2O$, 0.002 g/l; riboflavin, 0.005 g/l; and OL-6,8-thiocitic acid, 0.005 g/l. The trace element stock solution consisted of zinc sulfate$\cdot 7H_2O$, 0.1 g/l; manganese sulfate$\cdot H_2O$, 0.085 g/l; boric acid, 0.06 g/l; cobalt chloride$\cdot 6H_2O$, 0.02 g/l; cupric chloride, 0.004 g/l; nickel sulfate$\cdot 6H_2O$, 0.028 g/l; sodium molybdate$\cdot 2H_2O$, 0.04 g/l; and ferrous chloride, 0.3 g/l. The pH of the medium was adjusted to 7.0 ± 0.1 using HCl, 1 M.

16S rRNA Gene sequences of the sulfate-reducing isolate

DNA was extracted from centrifuged pellets using a FastDNA® Spin Kit for Soil (Qbiogene, Inc., CA). 16S rRNA genes were amplified using conventional PCR with primers 8f (5′-AGAGTTTGATCC TGG CTCAG) and 1492r (5′-GGTTACCTTGTTACGAC TT) (Operon Biotechnologies, Germantown, MD). The PCR products were purified using a QIAquick® Gel Extraction Kit (QIAGEN Sciences, MD) and Montage-PCR Filter Units (Millipore Corporation). The purified PCR products were sequenced by MCLab (South San Francisco, CA). High quality of the DNA sequencing result was obtained, indicating the high purity of the culture. The 16S rRNA

sequence was then compared to the GenBank sequence database using BLASTn search (National Center for Biotechnology Information, US). Genomic data of species closely related to the clones were imported to the MEGA3 software (Kumar et al. 2004) for sequence alignment. A phylogenetic tree was then constructed in the MEGA3 software using the neighbor joining algorithm with 500 bootstrapped replicates. The isolate was identified as a member of the *Desulfovibrio aerotolerans* species with a percent identity of 99%.

Growth kinetic characterization

Five replicate cultures of the sulfate-reducing isolate were grown at 30°C for 7 days in 80-ml of growth medium, as described previously, but with sodium bicarbonate at 5 mM. Each day for 7 days, 1.5-ml samples were assayed for ethanol and acetate, and 0.2-ml samples were diluted 500 times then assayed for hydrogen sulfide. At the conclusion of 7 days, 8-ml samples were saved for protein analysis. Pseudo second-order kinetics were then used to describe growth of the sulfate-reducing culture:

$$\frac{dX}{dt} = Y\,kSX; \tag{1}$$

$$\frac{dS}{dt} = -kSX. \tag{2}$$

$$Y = \frac{[\text{final protein concentration} - \text{initial protein concentration}](\text{mg protein/l})}{\text{Ethanol consumption over 7 days (mM)}}. \tag{3}$$

Biomass decay was assumed to be negligible over the timeframe of the experiment. Accordingly, the net growth yield (Y) was determined as:

Definitions of each parameter are provided in the Nomenclature section. Standard deviation of net growth yield was calculated using a first-order error propagation method. Non-linear regression was used to estimate the pseudo second-order rate constant, k. The ordinary differential equations (Eqs. 1 and 2 above) were solved with MATLAB. Ethanol concentrations over time were used to optimize the model fit. The coefficient of determination R^2 was determined as $R^2 = 1-(SS_{reg}/SS_{tot})$. SS_{reg} refers to the sum of the square of the differences between observed values and predicted values. SS_{tot} refers to the sum of the square of the differences between observed values and the mean. Uncertainty of the fitting parameter, k, was estimated after linearization. The first derivatives of all predicted values with respect to k were determined analytically and stored as a column in a Jacobian matrix, J. The mean square fitting error was estimated as:

$$\sigma_s^2 = \frac{1}{n-p}\sum \left(S_{\text{measured}} - S_{\text{predicted}}\right)^2 \tag{4}$$

where n is the number of total data points used for curve fitting, and p is the number of fitting parameters. The covariance, C, was then determined as $C = \sigma_s^2 * (J^T * J)^{-1}$. The standard deviation of k was given by $\sqrt{C}$.

The stoichiometric ratios of acetate production to ethanol consumption (r_A) and hydrogen sulfide production to ethanol consumption ($r_{sulfide}$) were estimated using non-linear regression. Predicted values of acetate concentrations at each time point were calculated as:

$$A_{\text{predicted}} = A_0 + r_A\left(S_0 - S_{\text{predicted}}\right). \tag{5}$$

Because hydrogen sulfide is present in both gaseous and aqueous phases, the moles of hydrogen sulfide species ($H_2S + HS^-$) in each serum bottle were estimated at each time point. The total moles of hydrogen sulfide species were thus expressed as:

$$M_T = M_T\left(f_{aq} + f_g\right) \tag{6}$$

where M_T is the total mole of hydrogen sulfide; f_{aq} is the fraction of hydrogen sulfide in the aqueous phase; and f_g is the fraction of hydrogen sulfide in the gas phase. The speciation of $HS^-_{(aq)}$ and $H_2S_{(aq)}$ at the pH of our experiment (a pH value near seven was maintained throughout the time course of the experiment) was estimated using visual MINTEQ software version 2.53 (Department of Land and Water Resources Engineering, KTH Royal Institute of Technology, Sweden). $H_2S_{(g)}$ was assumed to be in

equilibrium with $H_2S_{(aq)}$, allowing use of Henry's law to calculate the partial pressure of H_2S in the gas phase. The fraction of hydrogen sulfide in the aqueous phase (f_{aq}) can be expressed as:

$$f_{aq} = \frac{1}{1 + \left[\left(\frac{\text{gas volume (l)}}{R\left(\frac{\text{l·atm}}{\text{mol·K}}\right)T} \right) \left(\frac{f_{H_2S,aq}}{\text{liquid volume (l)}} \cdot \frac{k_H(\text{atm/mol fraction}) \cdot 18(\text{g/mol}) \cdot 1000(\text{l/m}^3)}{\rho_w(\text{kg/m}^3) \cdot 1000(\text{g/kg})} \right) \right]}. \quad (7)$$

The moles of hydrogen sulfide species predicted for each time point were calculated as:

$$\begin{aligned} \text{Sulfide}_{p,i} &= \text{Sulfide}_{p,i-1} \\ &- \left(\text{Sulfide}_{p,i-1} * f_{aq,i-1} * \frac{1.7(\text{ml})}{\text{liquid volume (ml)}} \right) \\ &+ r_{\text{Sulfide}} \left(S_{p,\text{mol},i-1} - S_{p,\text{mol},i} \right). \end{aligned} \quad (8)$$

The second term on the right hand side of Eq. 8 accounts for changes in gas and liquid volumes due to sampling, and was thus only included for the sample time points. We then determined the fitting parameters, r_A and $r_{sulfide}$, corresponding to the minimum values of the sum of the square of the differences between measured and predicted values. The coefficients of determination R^2 for the model fit of acetate and hydrogen sulfide data were determined as $R^2 = 1 - (SS_{reg}/SS_{tot})$.

With the estimated $r_{sulfide}$, we obtained a continuous curve of total moles hydrogen sulfide in a serum bottle over time in a manner similar to that described above using Eq. 8 but at smaller time intervals (0.01 day).

Electron equivalents of substrate (ethanol) and products (acetate, hydrogen sulfide and biomass) at all time points were calculated to determine the electron balance in the system. The losses of electron equivalents due to the sampling of the liquid phase were also computed and accounted for.

Figure 1 shows the fit of the pseudo second-order kinetics to ethanol, acetate, hydrogen sulfide, and protein measurement data. Table 1 summarizes the estimated kinetic parameters and stoichiometric ratio of acetate and hydrogen sulfide production to ethanol consumption. The net growth yield of sulfate reducing isolate (Y) observed in this study was 0.291 g protein/mol ethanol, which can be converted to 1.00 mgVSS/mmol ethanol using a conversion factor of 0.29 mg protein/mgVSS determined previously for the ancestor sulfate-reducing enrichment (Nyman 2006). The stoichiometric ratio of acetate produced to ethanol consumed was 0.94, while the stoichiometric ratio of hydrogen sulfide produced to ethanol consumed was 0.38.

Figure 2 illustrates the balance on electron equivalents over the sampling period. A fraction (12.6%) of the electrons was not accounted for. While corrections were made for liquid sampling, they did not explain this loss. The theoretical ratio of hydrogen sulfide produced to ethanol consumed is slightly <0.5, but the observed ratio was 0.38, again indicating loss of electron equivalents over time. The cause of this loss was not identified, but may have been due to hydrogen accumulation (not monitored).

Analytical techniques

U(VI) measurements were performed using a spectrofluorometer (Jobin Yvon Inc., Edison, NJ). Unless otherwise specified, all U(VI) measurements in this study include U(VI) in both aqueous and solid phases. U(VI) concentrations were analyzed with a spectrofluorometer (Jobin Yvon Inc., Edison, NJ). Fluorescence measurements of the uranyl-phosphate complexes were performed on diluted samples (1:30 in 10% phosphoric acid) at 515.4 nm emission acquisition mode and 280.0 nm excitation acquisition mode. The spectrofluorometer measurement used in this work is selective for U(VI). The detection limit for U(VI) was 0.01 ppm. The spectrofluorometer automatically repeats each measurement of fluorescence until the relative standard deviation of these measurements does not exceed 1%. The presence of

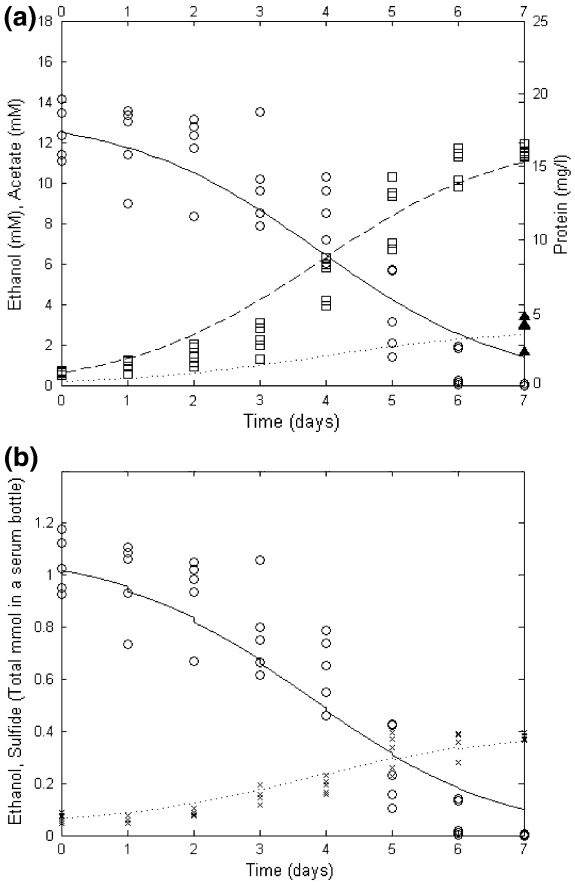

Fig. 1 Ethanol utilization, acetate production, hydrogen sulfide production, and microbial growth: **a** —, model fit of ethanol concentration (mM); – – – –, model fit of acetate concentration (mM); ….., model fit of protein concentration (mg/l); ○, measured ethanol concentration (mM); □, measured acetate concentration (mM); ▲, measured protein concentration (mg/l); **b** —, model fit of mole of ethanol in a serum bottle (mmol); ….., model fit of total mole of hydrogen sulfide in a serum bottle; ○, measured value of mole of ethanol in a serum bottle (mmol); ×, measured value of total mole of hydrogen sulfide in a serum bottle (mmol)

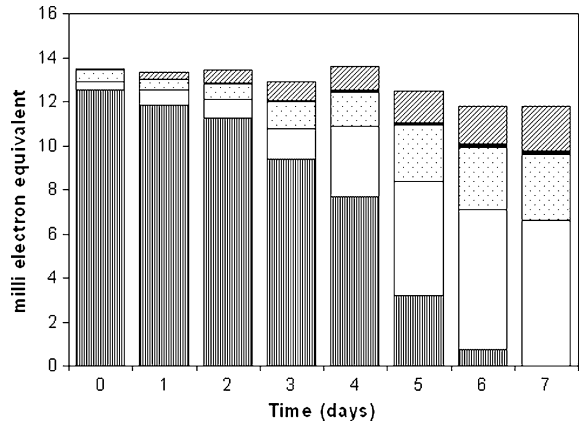

Fig. 2 Summation of electron equivalents in a serum bottle and electron lost over time: ▨, accumulated electron equivalents lost from liquid sampling; ■, electron equivalents in biomass; ⬚, electron equivalents in hydrogen sulfide; □, electron equivalents in acetate; ▥, electron equivalents in ethanol

anions and cations such as Cl^- and Co^{2+}, Cu^{2+}, Fe^{3+}, Mg^{2+}, and Mn^{2+} can interfere with the U(VI) measurements and can contribute to lower sensitivity, but standard curves for U(VI) were prepared using the uninoculated medium as background to eliminate potential interference. Ethanol and acetate concentrations were measured with a gas chromatograph outfitted with a flame ionization detector. Samples were prepared in 0.03 mM oxalic acid and directly injected into a packed column (80/120 Carbopack B-DA/4% CARBOWAX 20 M, HP5880, Supelco Inc., Bellefonte, PA; Nyman et al. 2006). Sulfate measurements were conducted using an ion chromatograph (Dionex, Sunnyvale, CA) fitted with an AS11-HC column. Protein concentrations in centrifuged pellets were measured using the Bradford assay (Bradford 1976). Hydrogen sulfide concentrations in the aqueous phase were analyzed with methylene

Table 1 Kinetic parameters and stoichiometric ratio of acetate and hydrogen sulfide production to ethanol consumption

Parameters	Best estimates ± SD	Units	R^2 for non-linear regression
Net growth yield (Y)	0.29 ± 0.08	g protein/mol ethanol	–
Pseudo second-order rate constant (k)	0.17 ± 0.16	l/mg protein/day	0.85
Stoichiometric ratio of acetate production to ethanol consumption	0.94	mol/mol	0.92
Stoichiometric ratio of hydrogen sulfide production to ethanol consumption	0.38	mol/mol	0.89

blue method using HACH-DR2800 (Hach company, Loveland, CO).

U(VI) reduction experiments

U(VI) reduction after growth of sulfate-reducing bacterium

The isolate was grown at 30°C for 6 days in two 150-ml serum bottles. Each bottle contained 100 ml of headspace filled with He and 50 ml of medium at two different bicarbonate levels: one level (5 mM) was chosen to approximate field conditions, and the other (15 mM) was chosen to give a value that was lower than previous laboratory studies.

The composition of the growth medium was the same as that described previously, but with a lower sulfate concentration (0.56 g/l) to ensure complete reduction of sulfate to sulfide before addition of U(VI). At the end of the 6 days, 10 mM ethanol was added. U(VI) reduction was then evaluated in replicate anaerobic culture tubes; three for each level of bicarbonate. Prior to testing of U(VI) reduction, the tubes (10 ml/tube) were capped, purged with helium and autoclaved. Sulfate-reducing culture was then transferred to the tubes and the pH adjusted to 7 ± 0.1 with 1 M HCl and 1 M NaOH. Uranyl acetate (0.15 ml of $\sim$15 mM uranyl acetate stock) was then injected to give an initial concentration of approximately 230 μM. U(VI) concentrations in the replicates were subsequently monitored over a 4-day period.

Abiotic control set 1: hydrogen sulfide-mediated abiotic U(VI) reduction in the presence of trace metals

U(VI) reduction in the absence of cells was assayed in replicate anaerobic tubes; three for each bicarbonate level (5 and 15 mM of $NaHCO_3$). These buffer solutions were designed to simulate the composition of the culture medium after growth of sulfate-reducing bacteria. Growth media described in the isolation and cultivation section was used as buffer at the two levels of bicarbonate. Sulfate was not included because the objective was to simulate spent sulfate-free medium to the extent possible. A solution of $Na_2S{\cdot}9H_2O$ ($\sim$0.1 M) was added to achieve a hydrogen sulfide concentration equivalent to that achieved during SRB growth. The amount of sulfide stock solution to add was determined by preparing a series of calibration standards, where the volume of added stock solution was plotted against the measured hydrogen sulfide concentration. Using this curve, 0.57 and 0.76 ml of $\sim$0.1 M $Na_2S{\cdot}9H_2O$ were added to achieve 1.97 and 2.71 mM of hydrogen sulfide—the same levels observed in culture tubes containing 5 and 15 mM bicarbonate, respectively. The pH of these U(VI) reduction assay tubes was then adjusted to 7 ± 0.1 using 1 M HCl, and uranyl acetate (0.15 ml of $\sim$15 mM uranyl acetate stock) was added. Changes in the U(VI) concentrations in replicate tubes were then monitored over a 4-day period.

Abiotic control set 2: hydrogen sulfide-mediated abiotic U(VI) reduction in the absence of trace metals

H_2S-mediated reduction of U(VI) was assayed in triplicate for bicarbonate concentrations of 5 and 15 mM using the protocol described above, but excluding trace metals from the medium.

Abiotic control set 3: trace metal reduction of U(VI) in the absence of hydrogen sulfide

Abiotic U(VI) reduction was evaluated in the presence of added trace metals at the concentrations of the original medium, but hydrogen sulfide was not added. U(VI) reduction was evaluated in triplicate test samples at 5 and 15 mM bicarbonate. The pH was adjusted to 7 ± 0.1. Uranyl acetate (0.15 ml of $\sim$15 mM uranyl acetate stock) was added, and U(VI) concentrations were then measured over a 4-day period.

Abiotic control set 4: hydrogen sulfide-mediated abiotic U(VI) reduction in the presence of $FeCl_2$

U(VI) reduction was evaluated in triplicate test samples in the presence of hydrogen sulfide and $FeCl_2$ at 5 and 15 mM bicarbonate using the same protocol previously used, but $FeCl_2$ was added at 24 μM, the Fe concentration of the original SRB medium. Other trace metals were excluded.

Abiotic control set 5: hydrogen sulfide-mediated abiotic U(VI) reduction in the presence of trace metals and 5 mM of bicarbonate

U(VI) reduction was evaluated in triplicate incubations in the same manner as the abiotic U(VI) reduction, i.e., at 5 mM bicarbonate and in the presence of hydrogen sulfide plus trace metals. A white/gray floc formed under these conditions. Consequently, levels of aqueous U(VI) were monitored (in addition to total U(VI)). Aqueous U(VI) samples were prepared by filtering 1-ml samples through 0.2 μm filters (Nalgene filter PES). Total and aqueous U(VI) concentrations were analyzed using a spectrofluorometer as described previously.

Abiotic control set 6: hydrogen sulfide-mediated abiotic U(VI) reduction in the presence of bicarbonate buffer only

U(VI) reduction was evaluated in triplicate incubations in the same manner as the abiotic U(VI) reductions described above. In this case, however, the experiments were conducted in the presence of bicarbonate buffer (5 and 15 mM) only. The pH was adjusted to 7 ± 0.1 using 1 M HCl. A white/gray floc formed under these conditions, similar to that noted in other abiotic experiments.

SEM and EDX analysis of the white/gray floc

Two different floc samples (Sample #1 and Sample #2) were prepared for SEM and EDX analysis. Sample #1 was the uranium floc generated in medium solution with 5 mM bicarbonate, 1.97 mM H_2S, phosphate, and trace metals; Sample #2 was the uranium floc generated in 5 mM bicarbonate buffer alone with 1.97 mM H_2S. After U(VI) addition, quiescent conditions were maintained for 6 h to approximate conditions previously shown to facilitate floc formation. Samples were then centrifuged in 1-ml eppendorf centrifuge tubes and the supernatant removed. To increase the size of the recovered pellets, the centrifuge and decanting process was repeated four more times with additional sample added each time. The flocs were then dewatered by freeze-drying. The dried powder was mounted onto a copper tape (for Sample #1) or onto a carbon tape (for Sample #2) that was attached to an aluminum stub for SEM/EDX analysis (Gu et al. 2003). A Hitachi S-4000 scanning electron microscope (SEM) operated at 10 kV and equipped with an energy dispersive X-ray (EDX) detector was used for direct imaging of floc samples. EDX enabled analysis of surface elemental composition of the floc samples at selected spots.

Results

U(VI) reduction in the presence and absence of the sulfate-reducing bacterium

During growth of the sulfate-reducing isolate, up to 3.05 mM hydrogen sulfide accumulated in the culture grown at 5 mM and up to 3.97 mM accumulated in the culture grown at 15 mM of bicarbonate. For the culture grown at 5 mM bicarbonate, the protein concentration increased from 0.3 to 10 mg/l. For the culture grown at 15 mM bicarbonate, the protein concentration increased from 0.2 to 4 mg/l. After 6 days of growth, sulfate concentrations in the culture grown at 5 and 15 mM were undetectable, confirming complete reduction of the added sulfate to sulfide. After transferring the SRB culture to replicate culture tubes to test for U(VI) reduction, the hydrogen sulfide concentration in the culture tubes with 5 mM bicarbonate was 1.97 ± 0.05 mM, while the hydrogen sulfide concentration in the culture tubes with 15 mM bicarbonate was 2.71 ± 0.39 mM.

Hydrogen sulfide-mediated abiotic U(VI) reduction was assayed at 5 and 15 mM bicarbonate for the same H_2S levels that the isolate had previously produced. The rates of U(VI) reduction for both cases were similar, but rates were slightly faster in the abiotic H_2S incubations for both bicarbonate levels tested (Fig. 3).

The kinetics of U(VI) reduction at 5 and 15 mM bicarbonate cannot be explained by first- or second-order kinetics: for 5 mM bicarbonate, the reduction was rapid during the first 6 h but stopped after 12 h; for 15 mM bicarbonate, reduction continued for 24 h, but at a much reduced rate. Possible explanations would include: (1) depletion of hydrogen sulfide or an additional (unknown) reactant, and (2) formation of a phase that prevents the reactants from reacting further. Measurements at the conclusion of the experiments indicated that significant levels of hydrogen sulfide remained. Other factors evidently led to the

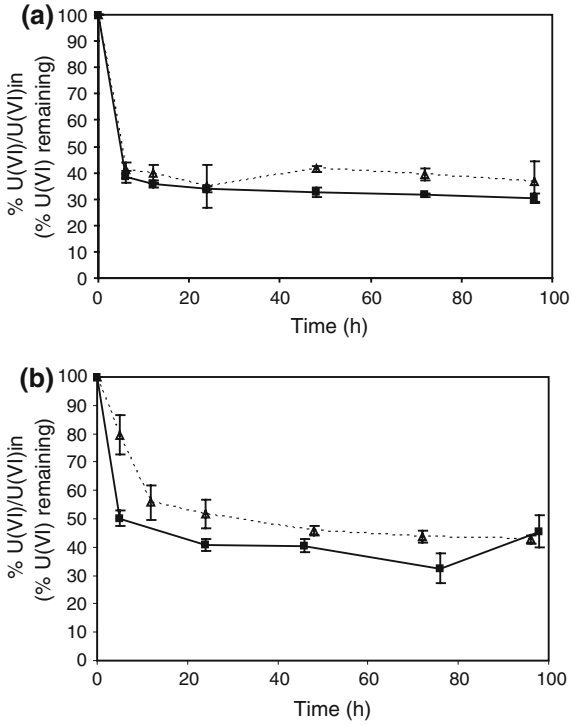

Fig. 3 U(VI) reduction in the presence and the absence of the sulfate-reducing isolate at **a** 5 mM bicarbonate and **b** 15 mM bicarbonate: - - Δ - -, U(VI) reduction in the presence of the sulfate-reducing isolate; —■—, hydrogen sulfide-mediated abiotic U(VI) reduction in the presence of trace metals. *Error bars* represent the standard deviations of three replicates

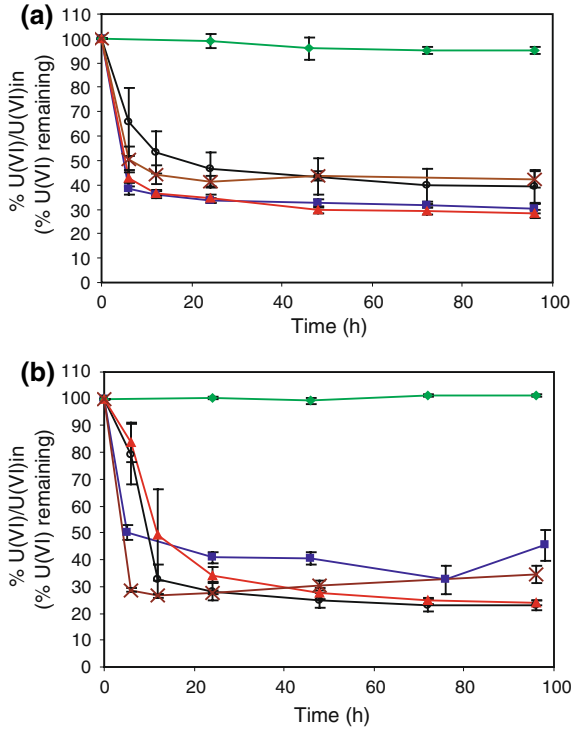

Fig. 4 Abiotic U(VI) reduction at **a** 5 mM bicarbonate and **b** 15 mM bicarbonate: —■—, hydrogen sulfide-mediated abiotic U(VI) reduction in the presence of trace metals; —o—, hydrogen sulfide-mediated abiotic U(VI) reduction in the absence of trace metals; —◆—, trace metal reduction of U(VI) in the absence of hydrogen sulfide; —▲—, hydrogen sulfide-mediated abiotic U(VI) reduction in the presence of $FeCl_2$; —X—, hydrogen sulfide-mediated abiotic U(VI) reduction in bicarbonate buffer (no PO_4^{3-}). *Error bars* represent the standard deviations of three replicates

cessation of U(VI) reduction. After 4–5 h of U(VI) reduction, a large amount of white/gray floc formed at 5 mM bicarbonate, and small amounts at 15 mM. The question was whether U(VI) was associated with the floc, and if so, whether it was resistant to reduction.

To test the possibility that one or more trace metal accelerated the initial reduction of U(VI) and that their depletion led to much slower reduction rates, rates of hydrogen sulfide-mediated abiotic U(VI) reduction were assayed in the absence of trace metals. The results were compared with the outcome of experiments performed in the presence of trace metals. The possibility of abiotic U(VI) reduction by trace metals in the absence of hydrogen sulfide was also evaluated. The results are shown in Fig. 4.

In the absence of added trace metals, U(VI) concentrations decreased gradually at 5 mM bicarbonate. The rapid drop in U(VI) concentrations that was observed in the presence of trace metals was not observed. This is consistent with the hypothesis that the trace metal addition enhanced U(VI) reduction. However, the difference of U(VI) reduction in the presence and absence of trace elements was small. At 15 mM bicarbonate, the difference of U(VI) reduction in the presence and absence of trace metals was unclear.

Trace metals alone did not have sufficient reducing power for U(VI) reduction: appreciable U(VI) reduction did not occur when trace metals were provided but not hydrogen sulfide.

Among all of the trace metals added to the medium for sulfate-reducing bacteria, $FeCl_2$ was added at the highest concentration (24 μM). Because iron can exist as Fe(II) or as Fe(III), it may be involved in redox reactions with U(VI). We therefore evaluated the effect of $FeCl_2$ alone on U(VI)

reduction. Figure 4 shows the results of the hydrogen sulfide-mediated abiotic uranium reduction in the presence of $FeCl_2$ at 5 and 15 mM of bicarbonate. At 5 mM of bicarbonate, the extent of U(VI) reduction was greater in the presence of Fe(II) or trace metals. The addition of Fe(II) appeared to enhance the extent of U(VI) reduction. On the other hand, at 15 mM bicarbonate, neither trace metals addition nor $FeCl_2$ addition led to a significant increase in U(VI) reduction by sulfide.

The possibility that cessation of U(VI) reduction might be due to U(VI) incorporation into the observed flocculent phase was investigated. The concentration of U(VI) in the heavy white/gray floc that formed at 5 mM bicarbonate was determined. Table 2 shows the concentrations of total U(VI) and aqueous U(VI) over time. After 6 h, aqueous U(VI) concentrations decreased to <4 μM. Figure 5 shows the Scanning Electron Microscopy (SEM) image and the Energy Dispersive X-Ray Spectroscopy (EDX) analysis of the floc samples removed from solution by centrifugation. The EDX results show that the floc contains uranium and co-precipitated sulfur, phosphorus, trace aluminum, trace silicon (an artifact of SEM/EDX analysis is a high background of copper due to the use of copper tape for the analysis). These solution and solid phase data indicate that over time, a large fraction of the U(VI) that disappeared from solution became associated with flocculent solids.

We also performed an experiment to test whether phosphate in the medium was responsible for the floc formation and the cessation of U(VI) reduction. U(VI) reduction was tested in bicarbonate buffer alone (at 5 and 15 mM bicarbonate). The results are shown in Fig. 4. Interestingly, after 4–5 h, white/gray floc still formed, and a similar pattern of U(VI) cessation was observed in the absence of added phosphate. As before, the amount of floc formed at 15 mM bicarbonate was less than that formed at 5 mM bicarbonate.

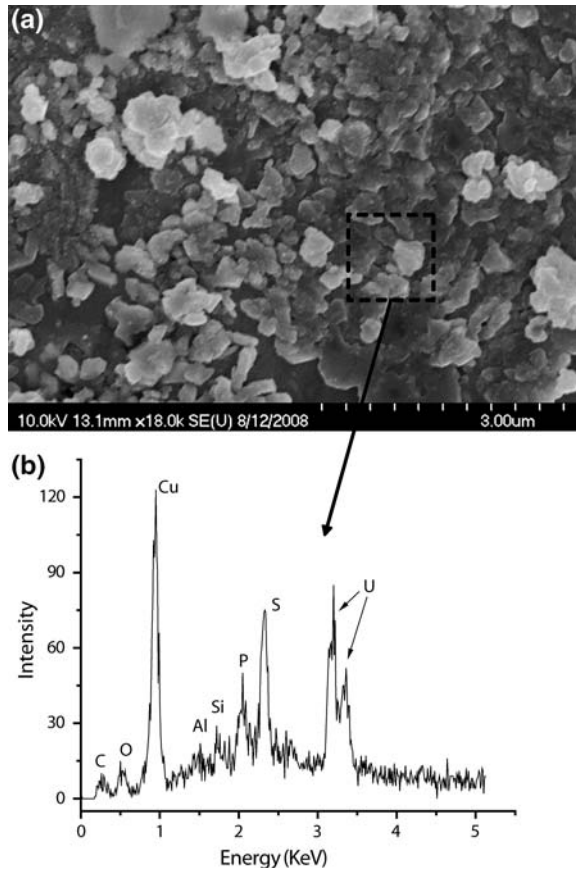

Fig. 5 **a** SEM image and **b** EDX analysis of the floc prepared in medium solution with 5 mM bicarbonate, 1.97 mM H_2S, phosphate, and trace metals (Sample #1)

Table 2 Hydrogen sulfide-mediated abiotic U(VI) reduction in the presence of trace metals at 5 mM of bicarbonate: total U(VI), aqueous U(VI) (0.2 μm filtrate), and U(VI) associated with the white/gray floc

Time (h)	Total U(VI) ± SD (μM) (1)	Aqueous U(VI) ± SD (μM) (2)	U(VI) associated with the floc ± SD (μM) (1)–(2)
0	189.4 ± 3.2	217.2 ± 4.1	−27.8 ± 5.2[a]
6	100.6 ± 3.8	2.7 ± 1.2	97.9 ± 4.2
12	106.9 ± 9.0	2.6 ± 2.3	104.3 ± 9.3
24	113.4 ± 2.0	2.9 ± 2.3	110.5 ± 3.0
48	102.8 ± 3.9	0.3 ± 0.5	102.5 ± 4.0
72	117.6 ± 6.0	3.2 ± 1.3	114.4 ± 6.1

[a] Turbidity in the unfiltered sample interfered the spectrofluorescence measurement

The results suggest that floc formation is likely associated with the production of elemental sulfur during U(VI) reduction by hydrogen sulfide species. The apparent role of reaction products in floc formation would explain the fact that a noticeable amount of floc did not immediately form, but became noticeable only after the reaction had progressed for a certain period of time (4–5 h). Figure 6 shows the Scanning Electron Microscopy (SEM) image and the Energy Dispersive X-Ray Spectroscopy (EDX) analysis of the floc sample prepared under this condition. The floc contained uranium, sulfur, chlorine, silicon, aluminum, and sodium. It should be noted that EDX results can vary greatly depending on sample heterogeneity. The chlorine can be attributed to the HCl added for pH adjustment. The results indicate that phosphorus need not be present for the formation of floc.

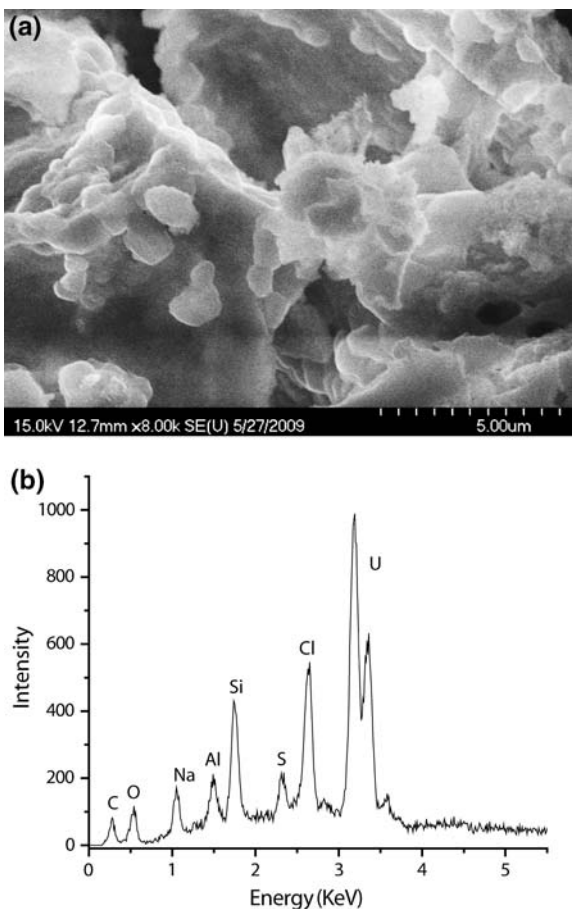

Fig. 6 **a** SEM image and **b** EDX analysis of the floc prepared in 5 mM bicarbonate buffer alone with 1.97 mM H_2S (Sample #2)

Discussion

Thermodynamics of U(VI) reduction by hydrogen sulfide

Table 3 gives the predicted speciation of uranyl, hydrogen sulfide, and phosphate species for the experimental systems used in this work (pH 7, with 5 mM or 15 mM bicarbonate) and at temperatures of 25 and 30°C. A speciation calculation was performed using the equilibrium software Visual MINTEQ version 2.53 and the associated thermodynamic database. At 5 and 15 mM bicarbonate, U(VI) speciation differs significantly at pH 7. At 30°C, uranyl phosphate was oversaturated at 5 mM bicarbonate, but undersaturated at 15 mM bicarbonate.

Table 4 summarizes free energy calculations for the reduction of different uranyl species by hydrogen sulfide at pH 7 and 25°C, for the concentrations given in Table 3. Enthalpy data needed for temperature correction to 30°C was not available for some species, so calculations were performed at 25°C. In previous research, Hua et al. (2006) observed that the stoichiometric ratio of U(VI) reduced to sulfide oxidized was 1:1, consistent with the assumption that elemental sulfur is the product of sulfide oxidation. Elemental sulfur is therefore assumed to be the product of sulfide oxidation for the equations in Table 4.

At 5 and 15 mM bicarbonate and a total initial U(VI) concentration of 230 μM, the reduction of most uranyl species ($UO_2(CO_3)_2^{2-}$, $UO_2(CO_3)_3^{4-}$, $UO_2HPO_{4(aq)}$, $UO_2PO_4^-$, and $(UO_2)_3(PO_4)_{2(s)}$) by hydrogen sulfide is thermodynamically favorable. Reduction of $UO_2(CO_3)_2^{2-}$, $UO_2(CO_3)_3^{4-}$, $UO_2HPO_{4(aq)}$, and $UO_2PO_4^-$ by hydrogen sulfide remains thermodynamically favorable at uranyl concentration as low as 1.5×10^{-8} μM. For the batch incubations performed in this study, U(VI) concentrations were always above 1.5×10^{-8} μM, suggesting that U(VI) reduction by hydrogen sulfide was thermodynamically favorable throughout the time course of the experiments.

U(VI) reduction in the presence and absence of the sulfate-reducing bacterium

Surprisingly, the U(VI) reduction mediated by *D. aerotolerans* can largely be explained by the hydrogen sulfide produced during growth. The rates

Table 3 The speciation calculation using the equilibrium software Visual MINTEQ version 2.53 and the associated thermodynamic database

Uranyl species	Concentrations and solid amount			
	25°C		30°C	
	5 mM bicarbonate	15 mM bicarbonate	5 mM bicarbonate	15 mM bicarbonate
$UO_2(CO_3)_2^{2-}$ (μM)	5.66	49.40	17.04	70.23
$UO_2(CO_3)_3^{4-}$ (μM)	3.83	141.83	8.91	155.23
$UO_2HPO_{4(aq)}$ (μM)	0.14	0.15	0.34	0.17
$UO_2PO_4^-$ (μM)	0.63	0.67	1.59	0.80
$(UO_2)_2CO_3(OH)_3^-$ (μM)	0.28	0.76	1.55	0.91
Other aqueous species (μM)	72.88	11.67	1.31	1.69
$(UO_2)_3(PO_4)_{2(s)}$ (μmol/l)	0.52	1.41	65.90	0.00
HS^- (mM)	1.00	1.39	1.07	1.49
$H_2S_{(aq)}$ (mM)	0.97	1.32	0.90	1.22
HPO_4^{2-} (mM)	0.33	0.40	0.34	0.42
$H_2PO_4^-$ (mM)	0.43	0.47	0.43	0.48

Note: Total U(VI) concentration = 230 μM; Total phosphate concentration = 0.9 mM; $[H_2S]_{Total}$ = 1.97 mM at 5 mM bicarbonate; $[H_2S]_{Total}$ = 2.71 mM at 15 mM bicarbonate

Table 4 Free energy of U(VI) reduction by hydrogen sulfide at neutral pH

Reactions	$\Delta G_r'$ at	
	5 mM HCO_3^-	15 mM HCO_3^-
$1/2UO_2(CO_3)_2^{2-} + 1/4HS^- + 1/4H_2S + 1/4H^+ = 1/2UO_{2(s)} + 1/2S^0_{(s)} + HCO_3^-$	−26.8	−27.1
$1/2UO_2(CO_3)_3^{4-} + 1/4HS^- + 1/4H_2S + 3/4H^+ = 1/2UO_{2(s)} + 1/2S^0_{(s)} + 3/2HCO_3^-$	−27.4	−28.2
$1/2UO_2HPO_4 + 1/4HS^- + 1/4H_2S = 1/2UO_{2(s)} + 1/2S^0_{(s)} + 1/4HPO_4^{2-} + 1/4H_2PO_4^- + 1/2H^+$	−23.6	−23.9
$1/2UO_2PO_4^- + 1/4HS^- + 1/4H_2S = 1/2UO_{2(s)} + 1/2S^0_{(s)} + 1/4HPO_4^{2-} + 1/4H_2PO_4^-$	−23.6	−23.9
$1/2UO_2CO_3(OH)_3^- + 1/4HS^- + 1/4H_2S + 1/4H^+ = 1/2UO_{2(s)} + 1/2S^0_{(s)} + 1/4HCO_3^- + 3/4H_2O$	+767	+766
$1/6(UO_2)_3(PO_4)_{2(s)} + 1/4HS^- + 1/4H_2S = 1/2UO_{2(s)} + 1/2S^0_{(s)} + 1/6HPO_4^{2-} + 1/6H_2PO_4^- + 1/4H^+$	−37.2	−37.5

Note: $\Delta G_r'$ was corrected for the concentrations of each species as shown in Tables 3 and 4. ΔG_r^0 was calculated using thermodynamic data from Benjamin (2002) and Guillaumont et al. (2003)

and extents of U(VI) reduction in the presence and absence of SRB were similar, with slightly faster rates in the abiotic tests. The slight decrease in the U(VI) reduction rates and extent of reduction in the presence of cells could be due to adsorption of U(VI) or U(VI)-reducing agents to biomass, which might slow the abiotic reduction.

The SRB evaluated in this work, *Desulfovibrio aerotolerans*, originated from an enrichment in which it was the dominant bacterium, as indicated by a clone library. The enrichment was capable of reducing U(VI) in the absence of hydrogen sulfide (Nyman et al. 2007; Boonchayaanant et al. 2008). Others have also observed enzymatic reduction by *Desulfovibrio* spp. in the absence of hydrogen sulfide (Lovley and Phillips 1992a, b; Lovley et al. 1993a, b). These prior U(VI) reduction assays were conducted under non-growth conditions, i.e., cells were washed and resuspended in bicarbonate buffer together with an electron donor. U(VI) reduction occurred in the absence of sulfate and sulfide, indicating an enzymatic mechanism. It should be noted that SRB U(VI) reduction rates vary greatly (Lovley et al. 1993a), but under the conditions of this study (i.e., *D. aerotolerans* plus 5 and 15 mM bicarbonate), U(VI) reduction is largely abiotic.

At 5 mM of bicarbonate, the extent of U(VI) reduction was greater in the presence of Fe(II) or trace metals. The pattern kinetics of uranium reduction in the presence of $FeCl_2$ at 5 mM bicarbonate was similar to the pattern observed in the presence of the complete trace metal solution, suggesting that Fe(II) was responsible for enhanced U(VI) reduction at 5 mM bicarbonate. At 15 mM bicarbonate, however, there was little effect of $FeCl_2$ and trace metals addition. A possible explanation is that uranyl species at 5 and 15 mM bicarbonate differ in their susceptibility to reduction by H_2S and/or Fe(II). Moreover, given that the redox couples for Fe(II)/(III) and U(IV)/U(VI) are similar, it can be expected that the direction of the reaction is highly dependent on relative concentrations and chemical forms.

Previous studies have shown that Fe(II) and Fe(II) minerals, such as green rusts and amorphous iron sulfide (FeS), can reduce U(VI) at neutral pH though surface catalysts were required under certain conditions (Liger et al. 1999; O'Loughlin et al. 2003; Behrends and Van Cappellen 2005; Hua and Deng 2008). In our study, trace Fe(II) enhanced U(VI) reduction in the presence of hydrogen sulfide, but trace Fe(II) by itself did not. The formation of dissolved FeS may have occurred (saturation levels were not exceeded), and it may have reduced U(VI) at a faster rate than hydrogen sulfide itself. Alternatively, ferrous iron formed by sulfide reduction of Fe(III) may have reduced U(VI). Hydrogen sulfide might regenerate Fe(II) after its oxidation to Fe(III).

Tests of the floc that formed after 4–5 h at 5 mM bicarbonate revealed a large fraction of U(VI) associated with the white/gray floc. This U(VI) was not accessible for reduction. The observation that U(VI) reduction was faster in the absence of biomass than in its presence was also unexpected and at first appears counter-intuitive, but can be explained by a similar mechanism: partitioning into an inaccessible phase which may include the biomass itself. Sorption of U(VI) to biomass has been reported in previous studies (Haas et al. 2001; Bencheikh-Latmani and Leckie 2003; Kelly et al. 2001). At 15 mM, less floc formed, and the extent of transformation was somewhat greater.

Given that floc formation and concomitant cessation of U(VI) reduction occurred in the absence of phosphate, we conclude that U(VI) reduction is likely self-limiting and due to the formation of floc containing elemental sulfur formed during the reaction. This issue merits further investigation given the importance of sulfate reduction in bioreduced systems used for uranium remediation (Wu et al. 2006b).

Conclusion

Hydrogen sulfide-mediated abiotic U(VI) reduction is the dominant reduction mechanism for the conditions evaluated. At 5 mM bicarbonate, addition of trace levels of ferrous iron increased the extent of U(VI) reduction in the presence of hydrogen sulfide, but at 15 mM bicarbonate, the effect of ferrous iron addition was unclear. At 5 mM bicarbonate, a large fraction of the U(VI) removed from the aqueous phase became associated with a sulfur-containing white/gray floc preventing further U(VI) reduction. The interactions among U(VI), hydrogen sulfide, Fe(II), biomass, and solid phases that were observed in this study are also likely to exist in actual environments where typical bicarbonate concentrations are low (<5 mM). Future studies should, therefore, take into consideration the potential for such reactions, and their effects on the fate and transport of uranium in the subsurface.

Acknowledgments This work was funded by the Environmental Remediation Science Program (ERSP), U.S. Department of Energy, under grant number DOEAC05-00OR22725. We thank two anonymous reviewers for thoughtful reviews and recommendations that significantly improved the manuscript.

References

Anderson RT, Lovley DR (2002) Microbial redox interactions with uranium: an environmental perspective. In: Keith-Roach MJ, Livens FR (eds) Interactions of microorganisms with radionuclides. Elsevier, Oxford, pp 205–223

Anderson RT, Vrionis HA, Ortiz-Bernad I, Resch CT, Long PE, Dayvault R, Karp K, Marutzky S, Metzler DR, Peacock A, White DC, Lowe M, Lovley DR (2003) Stimulating the in situ activity of geobacter species to remove uranium from the groundwater of a uranium-contaminated aquifer. Appl Environ Microbiol 69:5884–5891

Behrends T, Van Cappellen P (2005) Competition between enzymatic and abiotic reduction of uranium (VI) under iron reducing conditions. Chem Geol 220:315–327

Bencheikh-Latmani R, Leckie JO (2003) Association of uranyl with the cell wall of *Pseudomonas fluorescens* inhibits metabolism. Geochim Cosmochim Acta 67(21):4057–4066

Benjamin M (2002) Water chemistry. McGraw-Hill, New York, p 668

Boonchayaanant B, Kitanidis PK, Criddle CS (2008) Growth and cometabolic reduction kinetics of a uranium- and sulfate-reducing *Desulfovibrio*/Clostridia mixed culture: temperature effects. Biotechnol Bioeng 99(5):1107–1119

Bradford MM (1976) A rapid and sensitive method for quantitation of microgram quantities of protein utilizing the principle of protein-dye-binding. Anal Biochem 72:248–454

Cardenas E, Wu W-M, Leigh MB, Carley J, Carroll S, Gentry T, Luo J, Watson D, Gu B, Ginder-Vogel M, Kitanidis PK, Jardine PM, Zhou J, Criddle CS, Marsh TL, Tiedje JM (2008) Microbial communities in contaminated sediments associated with bioremediation of uranium to submicromolar levels. Appl Environ Microbiol 74(12):3718–3729

Elias DA, Suflita JM, McInerney MJ, Krumholz LR (2004) Periplasmic cytochrome c_3 of *Desulfovibrio vulgaris* is directly involved in H_2-mediated metal but not sulfate reduction. Appl Environ Microbiol 70(1):413–420

Francis AJ, Dodge CJ, Lu F, Halada GP, Clayton CR (1994) XPS and XANES studies of uranium reduction by *Clostridium* sp. Environ Sci Technol 28:636–639

Ganesh R, Robinson KG, Reed GD, Sayler GS (1997) Reduction of hexavalent uranium from organic complexes by sulfate- and iron-reducing bacteria. Appl Environ Microbiol 63(11):4385–4391

Gorby YA, Lovley YAG (1992) Enzymatic uranium precipitation. Environ Sci Technol 26:206–207

Gu B, Brooks SC, Roh Y, Jardine PM (2003) Geochemical reactions and dynamics during titration of a contaminated groundwater with high uranium, aluminum, and calcium. Geochim Cosmochim Acta 67:2749–2761

Gu BH, Wu WM, Ginder-Vogel MA, Yan H, Fields MW, Fendorf ZJ, Criddle CS, Jardine PM (2005) Bioreduction of uranium in a contaminated soil column. Environ Sci Technol 39:4841–4847

Guillaumont R, Fanghanel T, Neck V, Fuger J, Palmer DA, Grenthe I, Rand MH (2003) Update on the chemical thermodynamics of uranium, neptunium, plutonium, americium, and technetium. OECD Nuclear Energy Agency (ed) Elsevier, Amsterdam, The Netherlands, p 919

Haas JR, Dichristina TJ, Wade R Jr (2001) Thermodynamics of U(VI) sorption onto *Shewanella putrefaciens*. Chem Geol 180:33–54

He Z, Gentry TJ, Schadt CW, Wu L, Liebich J, Chong SC, Huang Z, Wu W, Gu B, Jardine P, Criddle C, Zhou J (2007) GeoChip: a comprehensive microarray for investigating biogeochemical, ecological, and environmental processes. ISME J 1:67–77

Hua B, Deng B (2008) Reductive immobilization of uranium(VI) by amorphous iron sulfide. Environ Sci Technol 42(23):8703–8708

Hua B, Xu H, Terry J, Deng B (2006) Kinetics of uranium (VI) reduction by hydrogen sulfide in anoxic aqueous system. Environ Sci Technol 40:4666–4671

Hwang C, Wu W-M, Gentry TJ, Carley J, Carroll SL, Watson D, Jardine PM, Zhou J, Criddle CS, Fields MW (2008) Bacterial community succession during in situ bioremediation of U(VI): spatial similarities along controlled flow paths. ISME J. Published on-line September 4

Kelly SD, Boyanov MI, Bunker BA, Fein JB, Fowle DA, Yee N, Kemner KM (2001) XAFS determination of the bacterial cell wall functional groups responsible for complexation of Cd and U as a function of pH. J Synchrotron Rad 8:946–948

Kumar S, Tamura K, Nei M (2004) MEGA3: integrated software for molecular evolutionary genetics analysis and sequence alignment. Brief Bioinform 5:150–163

Liger E, Charlet L, Van Cappellen P (1999) Surface catalysis of uranium(VI) reduction by iron(II). Geochim Cosmochim Acta 63:2939–2955

Lovley DR, Phillips EJP (1992a) Reduction of uranium by *Desulfovibrio desulfuricans*. Appl Environ Microbiol 58:850–856

Lovley DR, Phillips EJP (1992b) Bioremediation of uranium contamination with enzymatic uranium reduction. Environ Sci Technol 26:2228–2234

Lovley DR, Roden EE, Phillips EJP, Woodward JC (1993a) Enzymatic iron and uranium reduction by sulfate-reducing bacteria. Mar Geol 113:41–53

Lovley DR, Giovannoni SJ, White DC, Champine JE, Phillips EJP, Gorby YA, Goodwin S (1993b) *Geobacter metallireducens* gen. nov. sp. nov., a microorganism capable of coupling the complete oxidation of organic compounds to the reduction of iron and other metals. Arch Microbiol 159:336–344

McCullough J, Hazen TC, Benson SM, Metting FB, Palmisano AC (1999) Bioremediation of metals and radionuclides: what it is and how it works. Lawrence Berkeley National Laboratory, California

Nyman JL (2006) Community structure and kinetics of microbial uranium reduction for field-scale bioremediation. Dissertation, Stanford University, Stanford

Nyman JL, Marsh TL, Ginder-Vogel MA, Gentile M, Fendorf S, Criddle CS (2006) Heterogeneous response to biostimulation for U(VI) reduction in replicated sediment microcosms. Biodegradation 17:303–316

Nyman J, Wu H-I, Gentile M, Criddle CS (2007) Inhibition of a U(VI)- and sulfate-reducing consortia by U(VI). Environ Sci Technol 41:6528–6533

O'Loughlin EJ, Kelly SD, Cook RE, Csencsits R, Kemner KM (2003) Reduction of uranium(VI) by mixed iron(II)/iron(III) hydroxide (green rust): formation of UO_2 nanoparticles. Environ Sci Technol 37:721–727

Phillips EJP, Landa ER, Lovley DR (1995) Remediation of uranium contaminated soils with bicarbonate extraction and microbial U(VI) reduction. J Ind Microbiol 14:203–207

Pietzsch K, Babel W (2003) A sulfate-reducing bacterium that can detoxify U(VI) and obtain energy via nitrate reduction. J Basic Microbiol 43:348–361

Pietzsch K, Hard BC, Babel W (1999) A *Desulfovibrio* sp. capable of growing by reducing U(VI). J Basic Microbiol 39:365–372

Sani R, Peyton B, Smith W, Apel W, Peterson J (2002) Dissimilatory reduction of Cr(VI), Fe(III), and U(VI) by *Cellulomonas* isolates. Appl Microbiol Biotechnol 60:192–199

Spear JR, Figueroa LA, Honeyman BD (1999) Modeling the removal of uranium U(VI) from aqueous solutions in the

presence of sulfate reducing bacteria. Environ Sci Technol 33(15):2667–2675

Spear JR, Figueroa LA, Honeyman BD (2000) Modeling reduction of uranium U(VI) under variable sulfate concentrations by sulfate-reducing bacteria. Appl Environ Microbiol 66:3711–3721

Taylor DM, Taylor SK (1997) Environmental uranium and human health. Rev Environ Health 12:147–157

Wersin P, Hochella MF Jr, Persson P, Redden G, Leckie JO, Harris DW (1994) Interaction between aqueous uranium (VI) and sulfide minerals: spectroscopic evidence for sorption and reduction. Geochim Cosmochim Acta 58:2829–2843

Widdel F, Pfennig N (1984) Dissimilatory sulfate-or sulfur-reducing bacteria. In: Krieg NR, Holt JG (eds) Bergey's manual of systematic bacteriology, vol 1, 9th edn. Williams & Wilkins, Baltimore, pp 663–679

Wu WM, Carley J, Fienen M, Mehlhorn T, Lowe K, Nyman J, Luo J, Gentile ME, Rajan J, Wagner D, Hickey RF, Gu B, Watson D, Cirpka OA, Kitanidis PK, Jardine P, Criddle CS (2006a) Pilot-scale in situ bioremediation of uranium in a highly contaminated aquifer. 1. Conditioning of a treatment zone. Environ Sci Technol 40:3978–3985

Wu WM, Carley J, Gentry T, Ginder-Vogel MA, Fienen M, Mehlhorn T, Yan H, Caroll S, Pace MN, Nyman J, Luo J, Gentile ME, Fields MW, Hickey RF, Gu B, Watson D, Cirpka OA, Zhou J, Fendorf S, Kitanidis PK, Jardine P, Criddle CS (2006b) Pilot-scale in situ bioremediation of uranium in a highly contaminated aquifer. 2. Reduction of U(VI) and geochemical control of U(VI) bioavailability. Environ Sci Technol 40:3986–3995

Wu WM, Carley J, Luo J, Ginder-Vogel M, Cardenas E, Leigh MB, Hwang C, Kelly SD, Ruan C, Wu L, van Nostand J, Gentry T, Lowe K, Melhourne T, Carroll S, Lou W, Fields MW, Gu B, Watson D, Kemner KM, Marsh TL, Tiedje J, Zhou J, Fendorf S, Kitanidis PK, Jardine PM, Criddle CS (2007) In situ bioreduction of uranium (VI) to submicromolar levels and reoxidation by dissolved oxygen. Environ Sci Technol 41:5716–5723